




**Ga[(NO₂A-N-(alfa-amino)propionate)] chelates: synthesis
and evaluation as potential tracers for ⁶⁸Ga PET**

Journal:	<i>Dalton Transactions</i>
Manuscript ID:	DT-ART-02-2014-000386.R1
Article Type:	Paper
Date Submitted by the Author:	28-Feb-2014
Complete List of Authors:	Martins, Jos  ; University of Minho, Chemistry Geraldes, Carlos; UNIV. OF COIMBRA, Life Sciences; Ferreira, Paula; University of Minho, Chemistry Ferreira, Miguel; University of Minho, Chemistry André, Joao; University of Minho, Chemistry Pereira, Maria; University of Minho, Chemistry Prata, Maria; University of Coimbra, IBILI,

Ga[(NO₂A-*N*-(α -amino)propionate)] chelates: synthesis and evaluation as potential tracers for ⁶⁸Ga PET

Miguel F. Ferreira,^a Goretti Pereira,^a João P. André,^a M. I. M. Prata,^b Paula M. T. Ferreira,^a José A. Martins,^{a*} Carlos F. G. C. Geraldes^{c,d}

^aCentro de Química (CQ-UM), Universidade do Minho, Campus de Gualtar, 4710-057 Braga, Portugal

^bICNAS and IBILI, Faculty of Medicine, University of Coimbra, 3000-548 Coimbra, Portugal

^cDepartment of Life Sciences, Faculty of Science and Technology, University of Coimbra, P.O. Box 3046, 3001-401 Coimbra, Portugal

^dChemistry Centre, University of Coimbra, Rua Larga, 3004-535 Coimbra, Portugal

Corresponding author: José A. Martins, Centro de Química, Campus de Gualtar, Universidade do Minho, 4710-057 Braga, Portugal. jmartins@quimica.uminho.pt.

Keywords: NO₂A-*N*-(α -amino)propionic acid chelators; Ga³⁺ complexes; ¹H and ⁷¹Ga NMR; ⁶⁷Ga³⁺-labelled chelates; serum stability; biodistribution

Abstract

The availability of commercial $^{68}\text{Ge}/^{68}\text{Ga}$ cyclotron-independent $^{68}\text{Ga}^{3+}$ generators is making Positron Emission Tomography (PET) accessible to most hospitals, which is generating a surge of interest in the design and synthesis of bi-functional chelators for Ga^{3+} . In this work we introduce the NO2A-*N*-(α -amino)propionic acid family of chelators based on the triazacyclononane scaffold. Complexation of the parent NO2A-*N*-(α -amino)propionic acid chelator and of a low molecular weight (model) amide conjugate with Ga^{3+} was studied by ^1H and ^{71}Ga NMR. The Ga^{3+} chelate of the amide conjugate shows pH-independent N_3O_3 coordination in the pH range 3-10 involving the carboxylate group of the pendant propionate arm in a 6 member chelate. For the Ga(NO2A-*N*-(α -amino)propionate) chelate, a reversible pH-triggered switch from Ga^{3+} coordination to the carboxylate group to coordination to the amine group of the propionate arm, was observed upon pH increase/decrease in the pH range 4-6. This phenomenon can conceivably constitute the basis of a physiological pH sensor. Both complexes are stable in the physiological range. The [^{67}Ga](NO2A-*N*-(α -benzoylamido)propionate) was found to be stable in human serum. Biodistribution studies of the $^{67}\text{Ga}^{3+}$ -labeled pyrene butyric acid conjugate NO2A-*N*-(α -pyrenebutanamido)propionic acid revealed that, despite its high lipophilicity and concentration-dependent aggregation properties, the chelate follows mainly renal elimination with very low liver/spleen accumulation and no activity deposition in bones after 24 hours. Facile synthesis of amide conjugates of the NO2A-*N*-(α -amino)propionic acid chelator, serum stability of the Ga^{3+} chelates and fast renal elimination warrant further evaluation of this novel class of chelators for PET applications.

Introduction

Endowing thermodynamically stable and kinetically inert metal chelates with conjugability is the subject of intense research given the plethora of properties offered by metal ions for imaging and therapy. Non-functionalised metal chelates exhibit high hydrophilicity, distribution into the interstitial compartment, fast renal clearance and featureless biodistribution profiles. Delivering metal chelates to injury sites, for imaging and/or therapeutic purposes, allows reducing the dose and background signals and minimizes potential harmful side effects on non target organs- especially critical with complexes of metal-radioisotopes.

Positron Emission Tomography (PET) is well established in clinical diagnostic for functional imaging thanks to its remarkably high detection sensitivity, relatively high spatial resolution and potential to quantify tracer uptake within lesions. ^{18}F , ^{11}C , ^{13}N are the most used radionuclides for PET imaging due to their positron emission properties and short lifetimes. These radionuclides are covalently incorporated into biomolecules (sugars, amino acids, etc) through chemical synthesis, starting from simple precursor molecules/ions generated in dedicated cyclotron units.¹ Molecules labeled with ^{11}C and ^{13}N are indistinguishable from the natural abundance stable isotope unlabelled molecules undergoing the same metabolic pathways. C-2 ^{18}F labeled glucose (2-Deoxy-2- ^{18}F]fluoroglucose- FDG) is the most widely used tracer in clinical PET imaging. Following uptake by the glucose transporters and phosphorylation, FDG is trapped inside cells as FDG-6-P, allowing visualization *in vivo* of glucose avid cells and tissues. ^{18}F decay allows the resulting 2- ^{18}OH]glucose to follow the normal glycolytic pathway.^{2,3} ^{18}F , and especially ^{11}C and ^{13}N -labelled PET tracers, half-lives of 109.8, 20.3, and 9.96 minutes, respectively, need to be produced *in loco* in dedicated cyclotron units, using fast, high yielding synthetic procedures coupled to expeditious purification schemes (operated remotely) to avoid substantial loss of activity.^{1,2,3} Many metal ion radionuclides (eg. $^{68}\text{Ga}^{3+}$, $^{64}\text{Cu}^{2+}$) also display positron emission properties suitable for PET imaging.⁴ Amongst these, $^{68}\text{Ga}^{3+}$, 89% positron branching accompanied by low photon emission (1077 keV, 3.22 %) and half live of 67.6 minutes, is suitable for labelling molecules with fast blood clearance.^{5,6} The commercial availability of $^{68}\text{Ge}/^{68}\text{Ga}$ cyclotron-independent $^{68}\text{Ga}^{3+}$ generators is making PET imaging available to most hospitals.⁷ Labeling (bio)molecules with metal ion radionuclides requires efficient pathways to attach covalently bi-functional chelators (post-conjugation labeling), or functionalized chelates (pre-conjugation labeling) to

biomolecules.^{4,5,6,7} High thermodynamic stability and kinetic inertness of the metal complexes is absolutely mandatory for safe and efficient PET imaging.^{8,9,10} Transferrin, the iron transport protein, is the main competitor for Ga^{3+} in serum given the similar ionic radius and coordination properties of Fe^{3+} and Ga^{3+} .¹¹ In addition to stability, fast complexation, ideally at room temperature, and efficient purification procedures of labeled conjugates, have to be taken into account in the design of new chelators for Ga^{3+} for use as PET tracers.¹² Moreover, complex formation with Ga^{3+} , obtained as $^{68}\text{GaCl}_3$ by elution of $^{68}\text{Ge}/^{68}\text{Ga}$ generators with diluted hydrochloric acid, must be carried out at pH values below 4 (usually in acetate or HEPES buffer) to avoid precipitation of Ga^{3+} as $\text{Ga}(\text{OH})_3$.^{13,14}

The coordination chemistry of Ga^{3+} is dominated by its hard character, preferring hard, charged base donors such as carboxylates, phosphonates and phosphinates in an octahedral geometry,¹⁰ although it has also been shown to have good affinity for thiolates, such as TACN-TM (TACN-TM = 1,4,7-triazacyclononane-*N,N',N''*-tris(mercaptoethyl)).^{10,15} Poly(aminocarboxylates) and poly(aminophosphonates/phosphinates) are the most efficacious chelators for Ga^{3+} . Macrocyclic, DOTA-type (DOTA= 1,4,7,10-tetrazacyclododecane-1,4,7,10-tetraacetic acid) and NOTA-type (NOTA= 1,4,7-triazacyclononane-1,4,7-triacetic acid) chelators form Ga^{3+} complexes displaying exceptional thermodynamic stability and kinetic inertness.^{12,16,17,18} Ga^{3+} complexes of linear, DTPA¹⁹ (DTPA= diethylenetetramine pentacetic acid) and EDTA-type²⁰ (EDTA= ethylenediaminetetraacetic acid) chelators were found to be kinetically too unstable for *in vivo* use, despite the high thermodynamic stability of its $\text{Ga}(\text{EDTA})^-$ and $\text{Ga}(\text{DTPA})^{2-}$ complexes.^{21,22} DOTA-monoamide (octadentate) chelators, developed originally as Gd^{3+} complexing agents for use as Contrast Agents (CA) for Magnetic Resonance Imaging (MRI), despite forming Ga^{3+} complexes exhibiting lower thermodynamic stability and higher kinetic lability than the parent $\text{Ga}(\text{DOTA})^-$ complex, are still kinetically inert enough for *in vivo* PET.¹² The peptide conjugate [^{68}Ga](DOTATOC) (DOTATOC = DOTA, Tyr³-octreotide) is worldwide used in hospitals for diagnostic of neuroendocrine tumors expressing somatostatin receptors.^{23,24} The macrocycle cavity of DOTA-type chelators, optimal for Ln^{3+} ions, is too big for Ga^{3+} complexation, originating distorted octahedral (N_4O_2) complexes.^{10,12,23,24} Good matching of the macrocycle cavity of NOTA with the ionic radius of Ga^{3+} results in $\text{Ga}(\text{NOTA})$ complexes exhibiting exceptional thermodynamic stability and kinetic inertness.^{16,17} Moreover, NOTA-type chelators display faster Ga^{3+} chelation kinetics at

lower temperatures than DOTA-type chelators.²⁵ NOTA-monoamide conjugates, although amenable through *facile* synthetic routes, are likely to result in complexes exhibiting lower thermodynamic stability and higher kinetic lability than their parent Ga(NOTA) complex, compromising their potential for biological applications.²⁶ Replacing an acetate arm on the NOTA scaffold, by an acetate group α -substituted with a reactive group, endows the NOTA scaffold with conjugability whilst preserving its N_3O_3 denticity mandatory for stable coordination with Ga^{3+} . The aspartate and glutamate derivatives of NOTA, NODASA (NODASA = 1,4,7-triazacyclononane-*N*-succinic-*N'*,*N''*-diacetic acid)²⁷ and NODAGA (NODAGA = 1,4,7-triazacyclononane-*N*-glutaric-*N'*,*N''*-diacetic acid)),²⁸ respectively, are the gold standards for the synthesis of targeted Ga^{3+} tracers for PET. More recently, the TRAP (TRAP = 1,4,7-triazacyclononane-1,4,7-tris(methylenephosphinic acid)) family of chelators, generated by replacement of the pendant carboxylates by phosphinate groups on the triazacyclononane macrocycle scaffold, revealed excellent chelating properties for Ga^{3+} allied to conjugability.^{29,30,31} *Tris*-NODASA/NODAGA³² and *tris*-TRAP²⁹ derivatives allow *facile* preparation of multivalent conjugates with biomolecules such as peptides, exhibiting enhanced avidity (affinity and/or specificity) for cellular receptors. Pendant reactive groups on the ethylenediamine bridges of the NOTA scaffold allow also bioconjugation whilst retaining the high thermodynamic stability and kinetic inertness of the Ga(NOTA) complex, although at the expense of difficult and lengthy synthetic pathways.³³

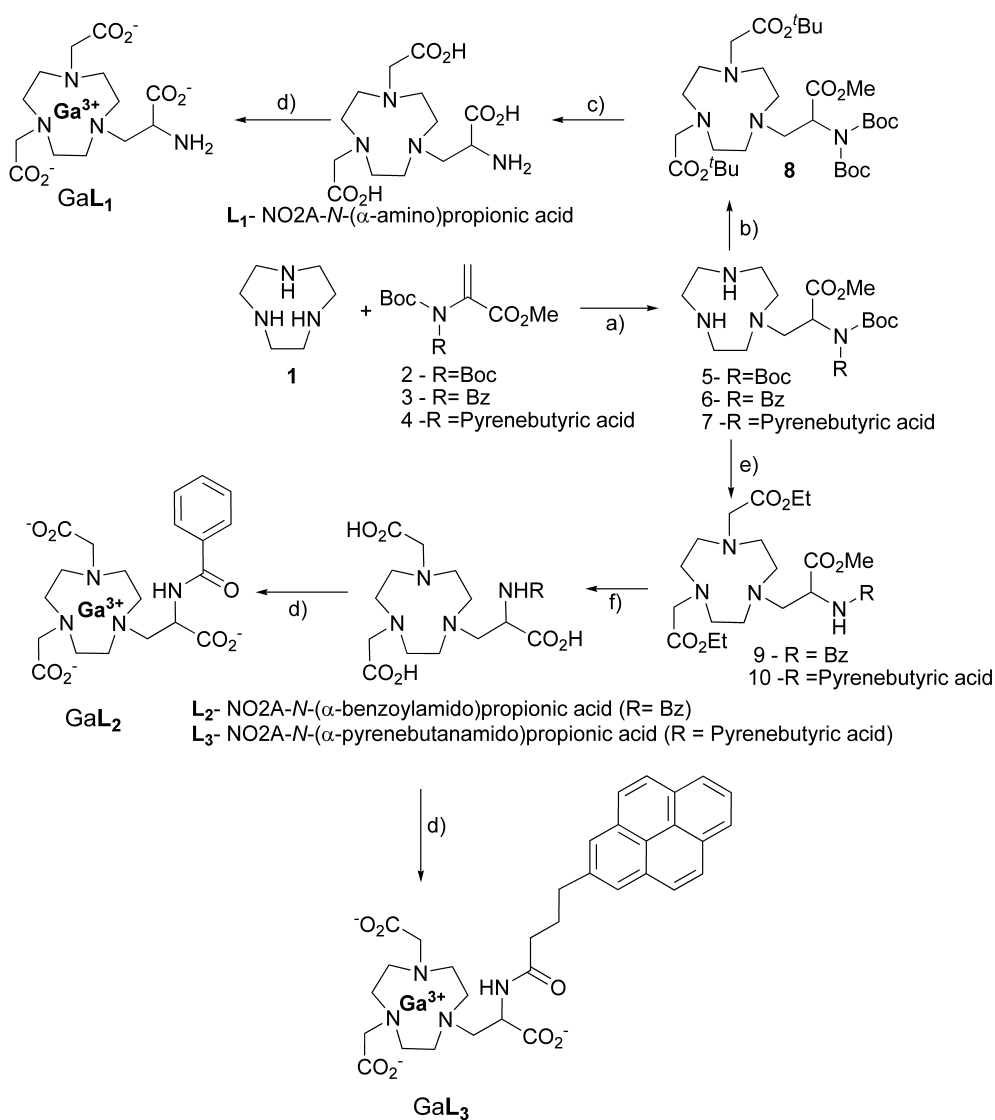
In our efforts to obtain thermodynamically stable and kinetically inert conjugates of metal chelates as potential medical imaging agents, we have reported recently efficient methodologies for the synthesis of the DO3A-*N*-(α -amino)propionate chelator³⁴ and for the preparation of amide conjugates.^{35,36,37} The Gd[DO3A-*N*-(α -amino)propionate] chelate and its amide conjugates, combine high thermodynamic stability and kinetic inertness with (fast) water exchange properties, ideal for attaining high relaxivities at (intermediate/high) fields relevant for Magnetic Resonance Imaging.^{34,35,36,37} In this work we extend the synthetic methodologies developed for DO3A-*N*-(α -amino)propionate chelators to the triazacyclononane scaffold. This includes the NO2A-*N*-(α -amino)propionic acid (**L**₁) chelator and the two amide derivatives NO2A-*N*-(α -benzoylamido)propionic acid (**L**₂) and NO2A-*N*-(α -pyrenebutanamido)propionic acid (**L**₃) (see Scheme 1). The complexation of the new chelators with Ga^{3+} was studied by

multinuclear NMR (^1H , ^{71}Ga). The luminescence properties of the GaL_3 complex were also analysed in order to evaluate its potential as a bimodal PET/optical imaging agent. Serum stability and biodistribution studies were also performed to evaluate the potential of the new chelators as $^{68}\text{Ga}^{3+}$ -labeled PET tracers.

Results and Discussion

Synthesis and Characterization

In this work we aimed at extending the synthetic methodologies developed for DO3A-*N*-(α -amino)propionate chelators^{34,35,36,37} to the triazacyclononane scaffold, to explore the coordination properties of NO2A-*N*-(α -amino)propionic acid chelators for Ga^{3+} as potential tracers for PET imaging (Scheme 1).



Scheme 1. Synthetic pathway for the metal chelators NO₂A-*N*-(α -amino)propionic acid (**L**₁), NO₂A-*N*-(α -benzoylamido)propionic acid (**L**₂) and NO₂A-*N*-(α -pyrenebutanamido)propionic acid (**L**₃)

a) K₂CO₃/MeCN; b) *tert*-Butyl bromoacetate, K₂CO₃/MeCN; c) i. Hydrochloric acid/EtOH, ii. Dowex-1X2-OH⁻, elution with diluted hydrochloric acid; d) GaCl₃·xH₂O; e) i. TFA/CH₂Cl₂; ii. Ethyl bromoacetate, K₂CO₃/MeCN; f) Dowex-1X2-OH⁻, elution with diluted hydrochloric acid.

Michael addition of the Boc₂- Δ -AlaOMe (**2**)³⁴ and Boc(Amide)- Δ -AlaOMe blocks **3**³⁶ and **4**³⁷ to triazacyclononane (**1**) proceeds smoothly in acetonitrile at room temperature, using K₂CO₃ as base, in 3-4 hours, as reported before for the *cyclen* analogue. An excess of triazacyclononane, 1.5 molar equivalents, affords the monoalkylated nonanes as main reaction products. Small amounts of *bis*- and *tris*-alkylated derivatives are easily removed by flash chromatography. Further *N*-alkylation of nonane **5** with *tert*-butyl bromoacetate, followed by sequential deprotection with hydrochloric acid (4 M) and Dowex1X2-OH⁻ resin, and elution with diluted hydrochloric acid afforded the NO₂A-*N*-(α -amino)propionic acid chelator (**L**₁) as hydrochloride in (non-optimised) 36% overall yield. Alkylation of monoalkylated *cyclen* **5** with ethyl bromoacetate offers the opportunity to deprotect selectively the amine group for further conjugation.³⁵ This (*direct*) conjugation pathway was not pursued in this work. Instead, we have explored the *indirect pathway* for preparing amide conjugates of the NO₂A-*N*-(α -amido)propionic acid chelator.³⁶ The NO₂A-*N*-(α -benzoylamido)propionic acid chelator (**L**₂) is likely to result in soluble non-associating chelates; the pyrenyl conjugate NO₂A-*N*-(α -pyrenebutanamido)propionic acid chelator (**L**₃) was designed as a self-assembling, fluorescent chelator, potentially useful for bimodal PET/fluorescence imaging.³⁷ Michael addition of Boc(dehydroamide)- Δ -AlaOMe blocks **3** and **4** introduces directly the amide (targeting/kinetic modulator) group into the triaza scaffold. Removing the Boc group at the monoalkylated stage averts retro-elimination during the second alkylation step. One step deprotection of the ester protected prochelators **9** and **10** with Dowex1X2-OH⁻ resin, affords the fully deprotected chelators **L**₂ and **L**₃ as hydrochlorides, after elution with aqueous hydrochloric acid.

Many other amide conjugates are accessible using the expeditious methodologies described in this work.

^1H and ^{71}Ga NMR studies

Given the current interest on ^{68}Ga PET, unleashed by the commercial availability of cyclotron-independent ^{68}Ga generators,^{4,5,6,7} we carried out a multinuclear NMR study (^1H and ^{71}Ga) of the GaL_1 and GaL_2 chelates to ascertain the coordination properties of the novel chelators and their potential for PET imaging applications.

^{71}Ga (38.89 %) is a quadrupolar nucleus ($I = 3/2$) exhibiting a relatively high receptivity and a wide range of chemical shifts.³⁸ The quadrupolar nature of its relaxation mechanism leads to NMR signals whose linewidth is sensitive to the symmetry of the coordination environment. Spherical, octahedral, cubic and tetrahedral symmetries should, in principle, originate sharp ^{71}Ga NMR signals. This is the case for NOTA-type triazamacrocyclic complexes, whose predominant coordination geometry is distorted octahedral, as opposed to DOTA-type tetraazamacrocyclic complexes like $\text{Ga}(\text{DOTA})$ - and its monoamide derivatives, whose low coordination symmetry makes their ^{71}Ga NMR signals to broad to be detected.¹² The chemical shift is characteristic of the coordination geometry of the metal ion.^{39,40}

The pH dependence of the ^1H (Figure 3) and ^{71}Ga NMR spectra (Figure 1) for the GaL_1 and GaL_2 complexes was studied in D_2O to probe the coordination environment of the Ga^{3+} metal ion.

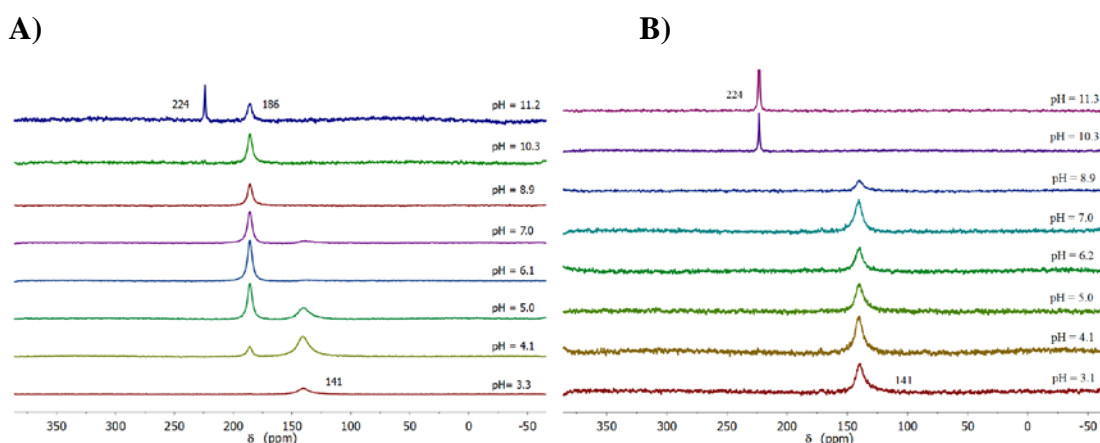


Figure 1. pH dependence of the ^{71}Ga NMR spectra for: (A) the GaL_1 and (B) GaL_2 complexes (400 MHz, 20 mM in D_2O , 25 °C).

Table 1 summarizes the ^{71}Ga NMR chemical shifts and linewidths for the species observed in solution for the GaL_1 and GaL_2 complexes studied in this work, compared with other triazamacrocyclic complexes reported in the literature (Figure 2).

Table 1. ^{71}Ga NMR chemical shifts and linewidths for the GaL_1 and GaL_2 complexes studied in this work, compared with other triazamacrocyclic complexes reported in the literature.⁴⁰

Complex	δ (ppm)	$\Delta\nu_{1/2}$ (Hz)	Coordination
GaL_1^a	+ 141	900	N_3O_3
	+ 186	550	N_4O_2
GaL_2^a	+ 140	900	N_3O_3
$\text{Ga}(\text{NOTA})^b$	+ 171	235	N_3O_3
$\text{Ga}(\text{NO}_2\text{A}-N\text{-Methylacetamide})^c$	+ 171	283	N_3O_3
	+ 175	9085	N_4O_2
$\text{Ga}(\text{NO}_2\text{A}-N\text{-Benzylacetamide})^c$	+ 170	279	N_3O_3
	+ 174	4818	N_4O_2
$\text{Ga}(\text{NOTP})^d$	+ 110	434	N_3O_3
$\text{Ga}(\text{NOTMP})^e$	+ 136	215	N_3O_3
$\text{Ga}(\text{TRAP-H})^f$	+ 132	154	N_3O_3
	+ 134	200	N_3O_3
	+ 138	186	N_3O_3
	+ 141	162	N_3O_3

^aThis work; ^bref. 17,41; ^cref. 42; ^dref. 43; ^eref. 44; ^fref. 30

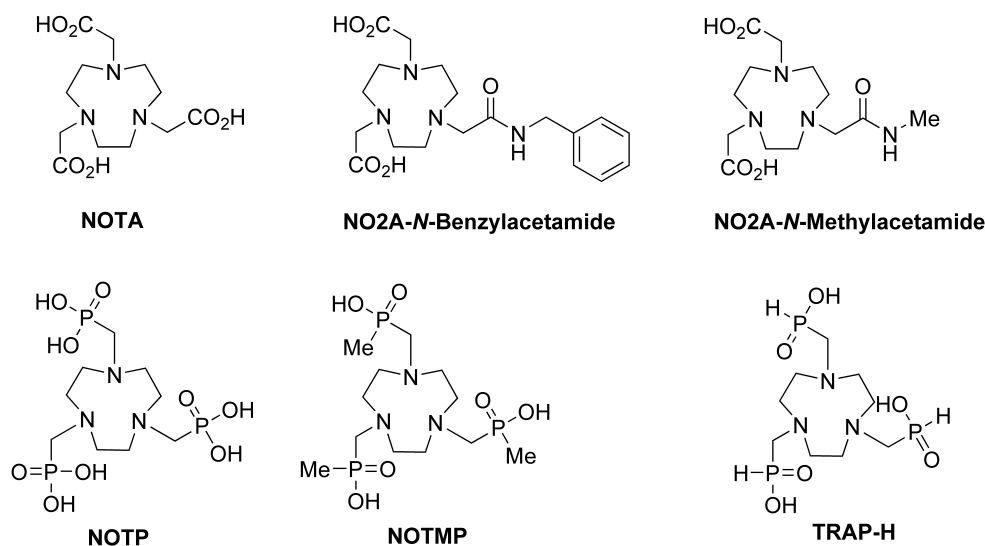


Figure 2. Structure of triazacyclononane ligands compared in Table 1 and discussed in the manuscript: NOTP (1,4,7-triazacyclononane- N,N',N'' -tris(methylenephosphonic) acid); NOTMP (1,4,7-triazacyclononane- N,N',N'' -tris(methylene(methylphosphinate))); TRAP-H (1,4,7-triazacyclononane-1,4,7-tris(methylenephosphonic acid)).

The number and population of the species present over the pH range 3-11, as well as their chemical shifts and linewidths are quite different for the GaL₁ and GaL₂ complexes.

The GaL₂ complex displays only one ⁷¹Ga NMR signal in the pH range 3-9: a singlet at $\delta = 140$ ppm with a relatively large linewidth, $\Delta\nu_{1/2} = 900$ Hz. Above pH 9.0, hydroxide catalyzed demetallation leads to the formation of the [Ga(OH)₄]⁻ species characterized by a sharp signal at $\delta = 224$ ppm.⁴⁰ In contrast, the ⁷¹Ga NMR spectrum of the GaL₁ chelate is pH dependent. At pH 3.0 there is only one signal with a chemical shift (141 ppm) and width (900 Hz) identical to that displayed by the GaL₂ complex. A new sharper ($\Delta\nu_{1/2} = 550$ Hz) signal at $\delta = 186$ ppm becomes apparent at pH 4.1. The intensity of this signal increases, at the expense of the signal at $\delta = 141$ ppm, when the pH increases, eventually becoming the only signal in the pH range 6-10. At pH 11, the [Ga(OH)₄]⁻ species is also present. This process is fully reversible, reproducing the same features upon pH decrease. These results strongly suggest that for the amide complex GaL₂, the coordination polyhedron is likely to be represented by a distorted octahedron involving the carboxylate group of the propionate arm to form a six member chelate (coordination polyhedron *N₃O₃*). Although coordination through the amide nitrogen, forming a five member chelate, is also possible, the preference of the hard Ga³⁺ ion for the carboxylate group is likely to compensate for the energy cost of forming a six member chelate.⁴² The GaL₁ chelate seems to undergo the same chelation scheme (*N₃O₃*) as the amide complex at low pH, presumably due to the unavailability of the protonated amine group for binding. At higher pH (6-11) the formation of a five member chelate with the deprotonated amine group (coordination polyhedron *N₄O₂*) seems to be more favorable than the formation of a six member chelate with the harder carboxylate group. The *N₄O₂* chelation mode for the GaL₁ chelate (all five member chelates) is likely to generate a coordination polyhedron of higher symmetry, similar to Ga(NOTA), than the *N₃O₃* geometry involving a six member chelate- thus, the sharper ⁷¹Ga NMR signal and higher chemical shift of the *N₄O₂* isomer of GaL₁ at pH 6-11. For the GaL₃ complex at 20 mM concentration, the ⁷¹Ga NMR spectrum becomes too broad to be measured, reflecting provably the micellar state of the complex.⁴⁵ Both GaL₁ and GaL₂ complexes are stable in the physiological pH range undergoing hydroxide catalyzed demetallation above pH 10 and 9, respectively. This is apparent in the ⁷¹Ga NMR spectra by the disappearance of the signals assigned to the complexes and by the

appearance of the sharp signal at $\delta = 224$ ppm, assigned to the $[\text{Ga}(\text{OH})_4]^-$ ion. All known Ga^{3+} complexes undergo hydroxide catalyzed demetallation in the alkaline pH region.⁴⁰ In this respect, the GaL_1 complex seems to be more stable than the amide conjugate GaL_2 chelate, requiring a higher pH for complete demetallation. This can be ascribed to the preference for the N_4O_2 coordination for the GaL_1 complex at high pH, compared to the N_3O_3 coordination of GaL_2 . A similar isomerization process involving coordination of the Ga^{3+} ion to the nitrogen or oxygen atom of the amide linkage (five member chelates), has been observed for the $\text{Ga}(\text{NO}_2\text{A-}N\text{-Benzylacetamide})$ and $\text{Ga}(\text{NO}_2\text{A-}N\text{-Methylacetamide})$ complexes (Figure 2 and Table 1), both in the solid state and in aqueous solution. At low pH the N_3O_3 coordination predominates over N_4O_2 coordination.⁴² As can be seen in Table 1, the two isomers of the $\text{Ga}(\text{NO}_2\text{A-}N\text{-Benzylacetamide})$ and $\text{Ga}(\text{NO}_2\text{A-}N\text{-Methylacetamide})$, involving in both cases five member chelates, show much smaller shift differences and are much broader than the isomers found in the present study for GaL_1 . The phosphonate complex $\text{Ga}(\text{NOTP})^{43}$ and some phosphinate complexes, like $\text{Ga}(\text{NOTMP})^{44}$ lead to the presence of only one species in solution. In all the NOTA-type complexes with N_3O_3 coordination the Ga^{3+} ion is placed between twisted trigonal O_3 and N_3 planes, an arrangement which leads to chiral complexes. This is caused by the combination of the conformation of the chelate rings in the macrocyclic moiety ($\delta\delta\delta/\lambda\lambda\lambda$) with the helicity of the coordinated pendant arms (Δ/Λ), which leads to two diastereoisomeric pairs $\Delta\delta\delta\delta/\Lambda\lambda\lambda\lambda$ and $\Lambda\delta\delta\delta/\Delta\lambda\lambda\lambda$. In the NOTA derivatives bearing three phosphinate pendant arms, those chiralities are combined with the *R/S* chirality of the phosphorus atom upon metal coordination, leading to four possible diastereomeric pairs, $\Lambda\delta\delta\delta - RRR/\Delta\lambda\lambda\lambda - SSS$, $\Lambda\delta\delta\delta - RRS/\Delta\lambda\lambda\lambda - SSR$, $\Lambda\delta\delta\delta - RSS/\Delta\lambda\lambda\lambda - SRR$ and $\Lambda\delta\delta\delta - SSS/\Delta\lambda\lambda\lambda - RRR$. In the Ga^{3+} phosphinate complexes with alkyl substituents (CH_3 in $\text{Ga}(\text{NOTMP})^{44}$ or CH_2OH in $\text{Ga}(\text{TRAP-OH})^{30}$, only the $\Lambda\delta\delta\delta - RRR/\Delta\lambda\lambda\lambda - SSS$ diastereoisomer is observed in solution, leading to a single ^{71}Ga signal, while for more electron-withdrawing substituents, like H in $\text{Ga}(\text{TRAP-H})^{30}$, the full mixture of possible isomers is observed in solution as a set of four narrow resonances with very small shift differences (Table 1).

The 1D ^1H and 2D COSY and NOESY spectra of the GaL_1 complex solutions were also obtained at 25 °C in the pH 3.0-9.0 range, and at pH 3.0-5.5 for GaL_2 . The proton resonance signals from the macrocyclic backbones were only tentatively

assigned due to superimposed multiplet signals in the 3.7-2.8 ppm range (Figures S1 and S2). The $\text{NCH}_2\text{CO}_2\text{H}$ acetate arm protons give a multiplet at 3.85 ppm, while the phenyl group of GaL_2 originates three multiplets at 7.70, 7.45 and 7.40 ppm with a 2:2:1 intensity ratio, corresponding to the *ortho*, *para* and *meta* CH protons. The most informative resonances correspond to the NCH_2CH protons of the substituted propionate arm of the complexes, in the form of a characteristic ABX pattern, with the CH proton resonances outside the envelope of the other protons (Figures S1 and S2). The AB patterns of the CH_2 signal coupled to the CH group (NCH_2CH) could be traced in the COSY spectra of both complexes (Figures S1 and S2). In the case of GaL_2 the CH multiplet has a single component at 5.05 ppm (Figure 3), in accordance with the single ^{71}Ga resonance at +140 ppm, corresponding to N_3O_3 coordination (Figure 1). In the case of GaL_1 the CH proton signals are pH-dependent, in parallel with what was observed for the ^{71}Ga NMR spectra (Figure 3). While at pH 3.3, it consists of a single multiplet (doublet of triplets) at 4.47 ppm (labeled I), corresponding to the single ^{71}Ga resonance at 141 ppm (N_3O_3 coordination isomer), at pH 4.1 there are two CH multiplets at 4.50 (I) and 4.38 ppm (II), corresponding to the ^{71}Ga signals at 141 and 186 ppm, assigned to the N_3O_3 and N_4O_2 isomers, respectively. The relative intensity of the N_4O_2 signals (4.38 ppm and 186 ppm) increases with pH in relation to the N_3O_3 signals (4.50 and 141 ppm) and at pH 6.1 only the 4.38 ppm signal is present. The corresponding CH_2 multiplets are observed between 3.60 and 3.20 ppm (Figures S1 and S2). Therefore, the proton NMR spectra confirm the isomer information provided by the ^{71}Ga NMR spectra.

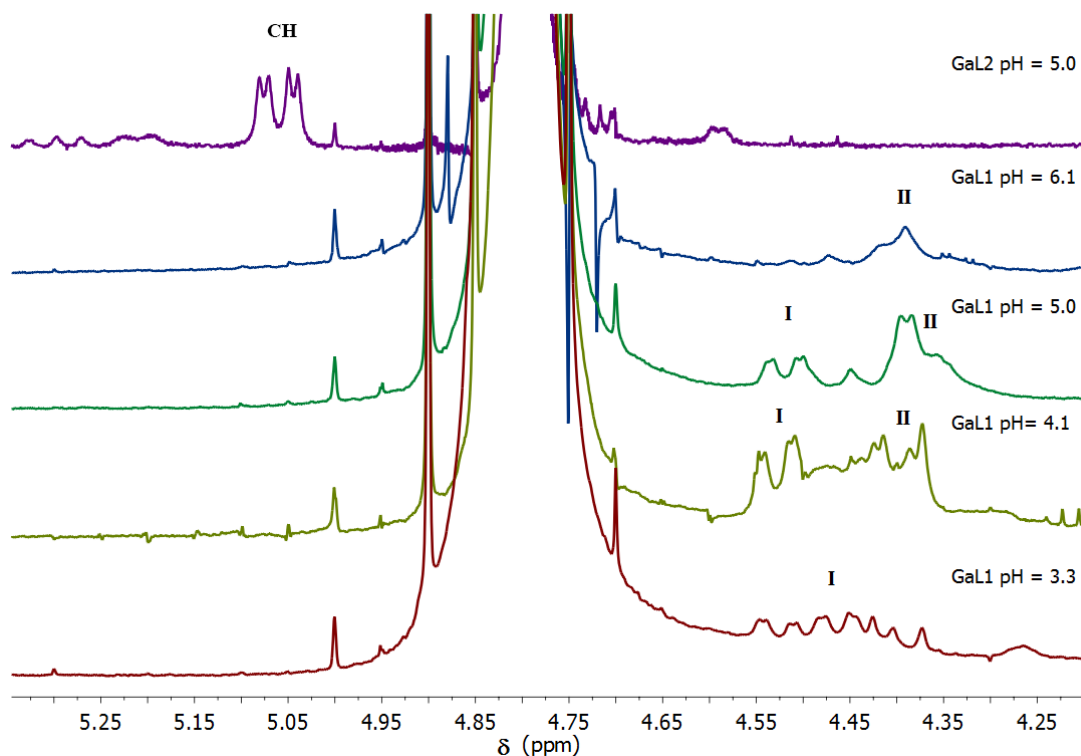


Figure 3. pH dependence of the proton NMR resonances of the CH protons of the propionate side arm of the GaL₁ and GaL₂ complexes (400 MHz, 20 mM in D₂O, 25 °C).

Fluorescence studies

The GaL₃ complex was designed to have properties compatible with a bimodal PET/Fluorescence imaging agent. The lipophilic pyrene moiety was selected due to its special aggregation-sensitive fluorescence properties.^{37,46} The absorption (Figure S3) and the fluorescence emission properties (Figure S4) of the free ligand L₃ and of the GaL₃ complex (Figure 4) were studied in non-deoxygenated water (pH 7.0) by UV-Vis and steady-state fluorescence spectroscopy (Table 2).

Table 2. Quantum yields (Φ_F) for the ligand L₃ and GaL₃ complex (λ_{ex} 345 nm) in non-deoxygenated water.

$\Phi_F^{a,b}$	
L ₃	GaL ₃
0.20	0.30

^aRelative to anthracene in ethanol ($\Phi = 0.27$)

^bLigand and complex at 1.0×10^{-6} M concentration, non-deoxygenated solutions

The absorption spectra of **L**₃ and Ga**L**₃ (1×10^{-5} M, pH 7.0) exhibit bands in the wavelength range 300-350 nm characteristic of pyrene intraligand $\pi-\pi^*$ transitions (Figure S3).⁴⁷ The steady state fluorescence spectra of **L**₃ (Figure S4) and Ga**L**₃ (Figure 4) at low micromolar concentrations (1×10^{-6} M, $\lambda_{\text{exc}} = 345$ nm) display the typical vibronically structured band, attributed to the pyrene monomer ($^1\pi-\pi^*$ transitions).^{37,48} The fluorescence quantum yields for **L**₃ and for the pyrene-centred emission in Ga**L**₃ are of the same order of magnitude as those reported for other pyrene conjugates.^{37,47,48} Complex formation with diamagnetic Ga³⁺ enhances slightly the fluorescence quantum yield of **L**₃. The concentration dependence of the steady state fluorescence properties of **L**₃ (Figure S4) and Ga**L**₃ (Figure 4) indicate that both ligand and complex undergo self-assembly, presumably into micelle-type structures, in aqueous solution.

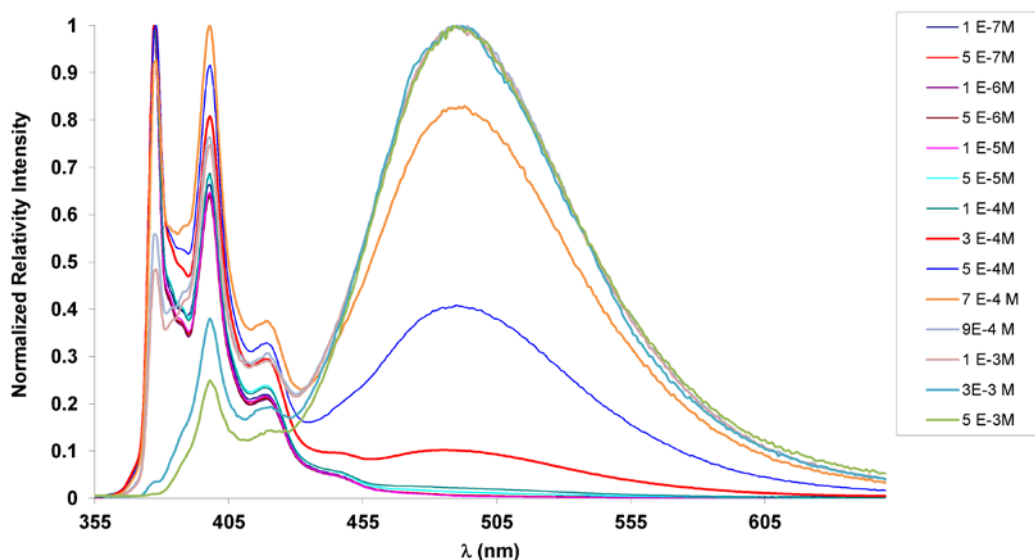


Figure 4. Normalized fluorescence spectra for Ga**L**₃ in non-deoxygenated water over the concentration range 5×10^{-7} - 5×10^{-3} mol.dm⁻³ ($\lambda_{\text{exc}} = 345$ nm).

Increasing the concentration of **L**₃ and Ga**L**₃ triggers a gradual switch from the characteristic structured pyrene monomer spectrum to the broad featureless typical excimer (excited dimer) spectrum, indicating self-assembly in solution, presumably in the form of micelle-type structures.³⁷ Attempts to calculate the critical micelle concentration (*cmc*) for **L**₃ and Ga**L**₃, by fitting the concentration dependence of the ratio of fluorescence emission intensity for the *excimer* (490 nm) and for the monomer (377 nm) (I_E/I_M), to a sigmoidal curve model revealed unsuccessful.^{37,49,50} Nonetheless, the aggregation-sensitive nature of the fluorescence emission is clearly observable.

Above the *cmc* aggregates coexist with the monomer at the *cmc* concentration. Increasing ligand or chelate concentration leads to an increase of the number of micelles enhancing excimer emission.

***In vitro* stability and biodistribution studies**

The kinetic stability of the [^{67}Ga] L_2 chelate towards *in vivo* transchelation was assessed by incubating the $^{67}\text{Ga}^{3+}$ -labeled chelate with fresh human serum, followed by precipitation of the protein fraction and measurement of the activity in the pellet and in the soluble fraction (Figure 5).

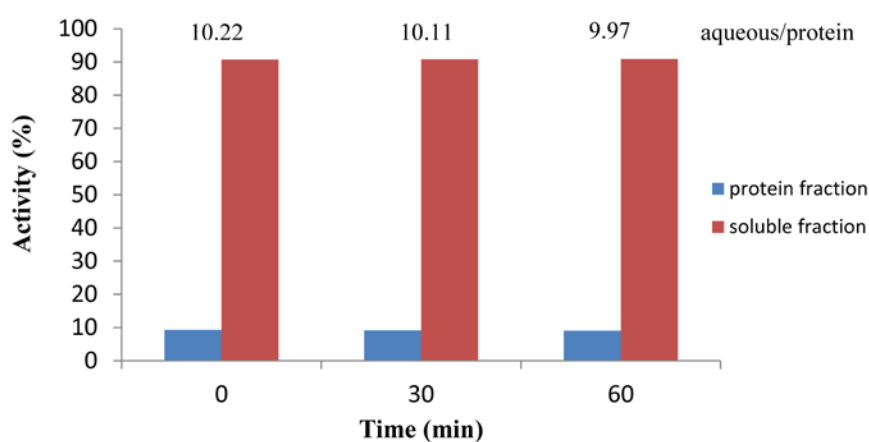


Figure 5. Percentage of activity in the protein and in the soluble fraction at different incubation times of [^{67}Ga] L_2 with human serum.

The percentage of total activity in the protein pellet reached immediately a value of 10% after incubating the complex with serum. This value remained constant over 1 hour incubation, revealing early association of the complex with blood proteins, presumably involving the lipophilic benzoyl moiety ($\text{Log } P_{\text{calculated}}(\text{GaL}_2) = 0.69$, see SI). Radio-TLC analysis of the soluble fraction after 1 hour incubation revealed that the complex remains intact.

Biodistribution profiles were obtained for the [^{67}Ga] L_3 labelled complex at 1 and 24 hour post-injection in Wistar rats (Figure 6, Table S1).

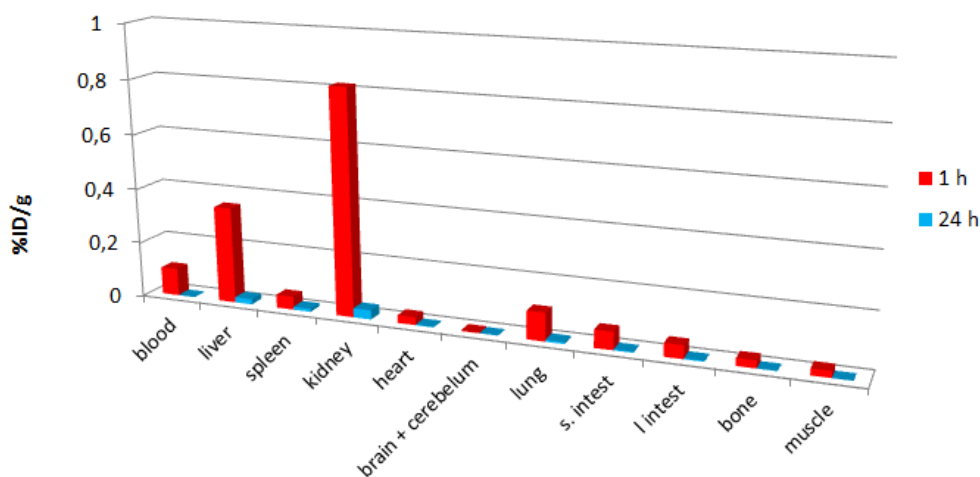


Figure 6. Biodistribution profiles, presented as % injected activity per gram of organ or tissue, for the $[^{67}\text{Ga}]\text{L}_3$ complex at 1 and 24 hours post-injection. Results are the average of 4 animals.

At 1 hour post-injection the activity is mainly located in the kidneys, liver and blood and to a lesser extent in the lungs and intestine. The high kidney uptake, comparing to liver, indicates that the main elimination pathway is renal. The relatively high activity in the blood at 1 hour post injection suggests association of the complex with plasma proteins, probably albumin or lipoproteins, presumably through the lipophilic pyrene moiety ($\text{Log } P_{\text{calculated}}(\text{GaL}_3) = 3.31$, see SI).³⁷ The very low spleen and lung uptake suggests that in the blood the complex is not aggregated. A motivating factor for performing the biodistribution study, was to ascertain potential brain uptake of GaL_3 . Biodistribution studies of the analogous $[^{153}\text{Sm}]\text{DO3A-N}-(\alpha\text{-pyrenebutanamido})\text{propionate}$ complex, suggested a low, although not negligible, activity uptake at the brain-cerebellum at 1 hour pi.³⁷ The higher lipophilicity of GaL_3 (overall neutral complex), comparing to its DOTA analogue $\text{Sm}(\text{DO3A-N}-(\alpha\text{-pyrenebutanamido})\text{propionate})$ complex (overall charge -1), could conceivably result in higher brain uptake. The current study excludes brain uptake of $[^{67}\text{Ga}]\text{L}_3$. Most importantly, no significant activity remains in the liver and spleen and there is no activity deposition in the bones after 24 hours, indicating that complex demetallation is not occurring *in vivo*.

Conclusions

In this work we extend the synthetic pathways, reported previously for the DO3A-*N*-(α -amino)propionate family of chelators, to the triazacyclononane scaffold. A reversible pH-triggered switch from Ga³⁺ coordination to the carboxylate group of the substituted propionate arm (at pH values below 4.0) to amine coordination (at pH values above 6.0), was uncovered by ¹H and ⁷¹Ga NMR studies of the Ga(NO2A-*N*-(α -amino)propionate) complex. The Ga³⁺ chelate of the benzoylamide conjugate displays pH-independent Ga³⁺ complexation to the carboxylate of the amide-substituted propionate arm in the pH range 3-11. Both complexes are stable in the physiological pH range. Moreover, the [⁶⁷Ga](NO2A-*N*-(α -benzoylamido)propionate) chelate is also stable in human serum. The pyrenebutyric acid conjugate, Ga(NO2A-*N*-(α -pyrenebutanamido)propionate) chelate, was designed as a potential bimodal PET/Fluorescence imaging agent with aggregation-sensitive fluorescence properties.

The facile synthesis of conjugates of the NO2A-*N*-(α -amino)propionic acid chelator, together with the serum stability of their Ga³⁺ chelates and fast renal elimination of the lipophilic pyrene conjugate, without any liver/spleen retention and activity deposition in the bones, warrant further evaluation of this novel class of chelators as potential tracers for PET. The reversible pH-triggered coordination switch demonstrated for the Ga(NO2A-*N*-(α -amino)propionate) complex can conceivably be translated into a method for pH measurement *in vivo* by ⁷¹Ga NMR.

Experimental

Materials and methods

Chemicals were purchased from Sigma-Aldrich and used without further purification. Analytical grade solvents were used without further purification, unless specified. Reactions were monitored by TLC on *Kieselgel*60 F254 (Merck) on aluminum support, with detection by examination under UV light (254 nm and 365 nm), by adsorption of iodine vapor and by spraying with ninhydrin. Flash chromatography was performed on *Kieselgel*60 (Merck, mesh 230-400). Ion exchange chromatography was performed on Dowex1X2-OH⁻ resin (Sigma Aldrich). The resin was purchased as the Cl⁻ form and converted to the OH⁻ form by the standard procedure. The relevant fractions from chromatography were pooled and concentrated under reduced pressure, T < 40 °C. ¹H

and ^{13}C NMR spectra (assigned by 2D DQF-COSY and HMQC techniques) were run on a Varian Unity Plus 300 and a Bruker Avance-3 400 Plus NMR spectrometers, operating at 299.938 MHz and 75.428 MHz, and 400.13 MHz and 100.61 MHz, for ^1H and ^{13}C , respectively. ^1H 1D and 2D DQF-COSY and NOESY spectra were also run on a Varian VNMRS 600 at 599.72 MHz. Chemical shifts (δ) are given in ppm relative to the CDCl_3 solvent (^1H , δ 7.27; ^{13}C 77.36) as internal standard. For ^1H and ^{13}C NMR spectra recorded in D_2O , chemical shifts (δ) are given in ppm, respectively, relative to TSP as internal reference (^1H , δ 0.0) and *tert*-butanol as external reference (^{13}C , CH_3 δ 30.29). ^{71}Ga NMR spectra were recorded at 122.026 MHz on a Bruker Avance-3 400 Plus spectrometer, using the signal of $[\text{Ga}(\text{H}_2\text{O})_6]^{3+}$ present in a 0.1 M $\text{Ga}(\text{NO}_3)_3$ solution in D_2O , at 0 ppm as external reference. pH measurements were performed on a pH meter Crison micro TT 2050 with an electrode Mettler Toledo InLab 422. For D_2O solutions, the isotopic correction $\text{pD} = \text{pH} + 0.4$ was done.⁵¹ Mass spectrometry was performed at CACTI- Vigo, Spain.

Synthetic procedures

Preparation of monoalkylated nonanes 5, 6 and 7.

Synthesis of bis(*tert*-butoxycarbonyl)amino-methoxycarbonylethyl-1,4,7-triazacyclononane- Monoalkylated nonane (5): $\text{Boc}_2\text{-}\Delta\text{-Ala-OMe}$ (**2**) (158 mg, 0.51 mmol) was added in one portion to a suspension containing 1,4,7-triazacyclononane (98 mg, 0.76 mmol) and K_2CO_3 (279 mg, 2.0 mmol) in MeCN (20 mL). The suspension was vigorously stirred at room temperature for 2 hours. The suspended solid was removed by filtration and the solvent was evaporated under reduced pressure. The residue was purified by flash chromatography (100% $\text{CH}_2\text{Cl}_2 \rightarrow \text{CH}_2\text{Cl}_2/\text{EtOH}/\text{NH}_4\text{OH}/\text{H}_2\text{O}$ (50:50:1:1)) to afford compound **5** (120 mg, 55 %). ^1H NMR (300 MHz, CDCl_3): δ = 1.51 (s, 18 H, Boc), 2.58-2.80 (m, 12 H, $\text{N}(\text{CH}_2)_2\text{N}$), 3.65 (dd, $J=14.1$ and 8.4 Hz, 1 H, ABX), 3.70 (dd, $J = 14.1$ and 4.5 Hz, 1 H, ABX), 3.71 (s, 3 H, $\text{C}(\text{O})\text{OMe}$), 5.01 (dd, $J=8.4$ and 4.5 Hz, 1 H, ABX). ^{13}C NMR (75.4 MHz, CDCl_3): 28.02 ($\text{C}(\text{CH}_3)_3$), 46.45 (CH_2), 46.83 (CH_2), 52.16 ($\text{C}(\text{O})\text{OCH}_3$), 53.16 (CH_2), 56.52 (CH_2), 56.67 (CH), 83.34 ($\text{C}(\text{CH}_3)_3$), 152.28 (C(O), carbamate), 170.73 (C(O), ester). HRMS (ESI): m/z : *calc*d for $\text{C}_{20}\text{H}_{39}\text{N}_4\text{O}_6$, $[\text{M}+\text{H}]^+$: 431.2864, found: 431.2859.

Synthesis of *N*-*tert*-butoxycarbonylbenzamido-methoxycarbonylethyl-1,4,7-triazacyclononane- Monoalkylated nonane (6): (benzyl)Boc- Δ -AlaOMe (**3**) (385 mg, 1.23 mmol) was added in one portion to a suspension containing 1,4,7-triazacyclononane (242 mg, 1.87 mmol) and K₂CO₃ (691 mg, 4.5 mmol) in MeCN (70 mL). The suspension was vigorously stirred at room temperature for 3 hours. The suspended solid was removed by filtration and the solvent was evaporated under reduced pressure. The residue was purified by flash chromatography (100% CH₂Cl₂ → CH₂Cl₂/EtOH/NH₄OH/H₂O (70:30:1:1)) to afford monoalkylated nonane **6** as a viscous light yellow oil (364 mg, 59 %). ¹H NMR (300 MHz, CDCl₃): δ = 1.47 (s, 9 H, C(CH₃)₃), 2.50-2.90 (m, 12 H, N(CH₂)₂N), 3.01 (dd, *J*= 14.1 and 6.0 Hz, 1 H, ABX), 3.49 (dd, *J*= 14.4 and 5.1 Hz, 1 H, ABX), 3.76 (s, 3 H, C(O)OMe), 5.25 (t, *J*= 6.0 and 5.1 Hz, 1 H, ABX), 7.30-7.70 (5 H, m, Ar). ¹³C NMR (75.4 MHz, CDCl₃): δ = 27.27 (C(CH₃)₃), 44.77 (CH₂), 45.83 (CH₂), 46.70 (CH₂), 51.27 (CH₂), 52.51 (C(O)OCH₃), 55.61 (NCH₂CH), 56.08 (CH), 83.88 (C(CH₃)₃), 127.87 (Ar), 127.96 (Ar), 131.27 (Ar), 137.02 (Ar), 152.72 (C(O), carbamate), 170.57 (C(O), amide), 172.62 (C(O), ester). HRMS (ESI): *m/z*: calcd for C₂₂H₃₅N₄O₅, [M+H]⁺: 435.2602, found: 435.2601.

Synthesis of methoxycarbonyl-(2-(*N*-*t*-butoxycarbonyl-4-pyrenebutanamido))-ethyl-4,7-bis-(ethoxycarbonylmethyl)-1,4,7-triazacyclononane- Monoalkylated 7: (Pyrenyl)Boc- Δ -AlaOMe (**4**) (1.01 g, 2.14 mmol) was added in one portion to a suspension containing 1,4,7-triazacyclononane (0.43 g, 3.33 mmol) and K₂CO₃ (1.76 g, 12.7 mmol) in MeCN (40 mL). The suspension was vigorously stirred at room temperature for 5 hours. The suspended solid was removed by filtration and the solvent was evaporated under reduced pressure. The residue was purified by flash chromatography (100% CH₂Cl₂ → CH₂Cl₂/EtOH/NH₄OH/H₂O (70:30:1:1)) to afford monoalkylated nonane **7** as a viscous light yellow oil (0.76 g, 59 %). ¹H NMR (300 MHz, CDCl₃): δ = 1.42 (s, 9 H, C(CH₃)₃), 2.21 (m, 2 H, NHC(O)CH₂CH₂), 2.64 (m, 8 H, 2xN(CH₂)₂N), 2.90 (m, 1 H, ABX), 3.12 (m, 6 H, N(CH₂)₂N and NHC(O)CH₂), 3.38-3.50 (m, 3 H, NHC(O)CH₂CH₂CH₂ and ABX), 3.43 (m, 2 H, N(CH₂)₂N), 3.70 (s, 3 H, C(O)OMe), 5.44 (t, *J*= 6.9 and 4.8 Hz, 1 H, ABX), 7.95-8.40 (9 H, m, Ar). ¹³C NMR (75.4 MHz, CDCl₃): δ = 27.03 (CH₂), 27.83 (C(CH₃)₃), 32.83 (CH₂), 37.85 (CH₂), 45.71 (CH₂), 46.20 (CH₂), 46.45 (CH₂), 52.11 (CH₂), 52.20 (C(O)OCH₃), 54.24 (CH), 58.17 (NCH₂CH), 84.34 (C(CH₃)₃), 123.44 (Ar), 123.87 (Ar), 124.72 (Ar), 125.02 (Ar), 125.76 (Ar), 126.58 (Ar), 127.28 (Ar), 127.47 (Ar), 128.66 (Ar), 129.85 (Ar), 130.82

(Ar), 130.92 (Ar), 131.33 (Ar), 151.86 (C(O), carbamate), 170.75 (C(O), ester). HRMS (ESI): m/z : calcd for $C_{35}H_{45}N_4O_5$, $[M+H]^+$, 601.3390, found: 601.3407.

Synthesis of *tris*-alkylated nonanes **8**, **9** and **10**

Synthesis of *bis*(*tert*-butoxycarbonyl)amino-methoxycarbonylethyl-4,7-*bis*-(*tert*-butoxycarbonyl methyl)-1,4,7-triazacyclononane- *tris*-alkylated nonane **8**: *tert*-

Butyl bromoacetate (85 μ L, 0.57 mmol) was added in one aliquot to a suspension containing monoalkylated compound **5** (100 mg, 0.23 mmol) and K_2CO_3 (125 mg, 0.90 mmol) in MeCN (20 mL). The suspension was vigorously stirred at room temperature for 3 hours. The suspended solid was removed by filtration and the solvent was evaporated under reduced pressure. The residue was purified by flash chromatography (100% $CH_2Cl_2 \rightarrow CH_2Cl_2/EtOH$ (50:50)) to afford *tris*-alkylated compound **8** (69 mg, 45 %). 1H NMR (300 MHz, $CDCl_3$): δ = 1.44 (s, 18 H, $C(CH_3)_3$, Boc), 1.65 (s, 18 H, $C(CH_3)_3$, ester), 2.75-3.78 (m(br) 12 H, $N(CH_2)_2N$), 3.03 (t, J = 4.2 Hz, 1 H, \underline{ABX}), 3.20 (t, J = 4.2 Hz, 1 H, \underline{ABX}), 3.73 (s, 4 H, $NCH_2C(O)$), 3.78 (s, 3 H, $C(O)OMe$), 5.01 (t, J = 4.2 Hz 1 H, \underline{ABX}). ^{13}C NMR (75.4 MHz, $CDCl_3$): 28.02 ($C(CH_3)_3$, Boc and t Bu ester), 44.53 (3 C, NCH_2CH_2 , CH_2), 50.80 (2 C, CH_2), 53.16 (2 C, CH_2), 52.33 (3 C, OCH_3 , 2 x CH_2), 56.52 (CH), 81.00 (2 C, $C(CH_3)_3$), 83.50 (2 C, $C(CH_3)_3$), 150.59 (1 C, $C(O)$), 151.98 (1 C, $C(O)$, carbamate), 163.95 (1 C, $C(O)OCH_3$), 170.98 (2 C, $C(O)$). HRMS (ESI): m/z : calcd for $C_{32}H_{59}N_4O_{10}$, $[M+H]^+$, 659.4226, found: 659.4218.

Synthesis of benzamido-methoxycarbonylethyl-4,7-*bis*-(ethoxycarbonylmethyl)-1,4,7-triaza cyclononane- *tris*-alkylated nonane **9**: A solution of monoalkylated compound **6** (340 mg, 0.78 mmol) in trifluoroacetic acid in dichloromethane (60%, 25 mL) was stirred overnight at room temperature. The solvent was evaporated at reduced pressure. The residue was re-dissolved in dichlorometane and the solvent was evaporated. This procedure was repeated several times to give a light yellow thick oil.

1H NMR spectroscopy ($CDCl_3$) revealed the disappearance of the signals assigned to the *Boc* group in the precursor compound. The oil (0.78 mmol, assuming quantitative deprotection) was dissolved in MeCN (30 mL), K_2CO_3 (1.0 g, 7.8 mmol) was added and the suspension was vigorously stirred at room temperature for 15 minutes. Ethyl bromoacetate (0.21 mL, 1.88 mmol) was added and the suspension was further stirred at room temperature for 2.5 hours. The suspended solid was removed by filtration, the solvent was evaporated under reduced pressure and the residue was purified by flash

chromatography (100% CH₂Cl₂ → CH₂Cl₂/EtOH (7:3)) to afford compound **9** (355 mg, 37 %) as a white foam. ¹H NMR (300 MHz, CDCl₃): δ= 1.22 (m, 6 H, C(O)OCH₂CH₃), 2.2-3.60 (broad multiplet, 18 H, N(CH₂)₂N, NCH₂C(O) and NCH₂CH), 3.71 (s, 3 H, C(O)OCH₃), 4.11 (t, *J*= 7.5 Hz, C(O)OCH₂CH₃), 5.14 (m (br), 1 H, NCH₂CH), 7.44-8.03 (5H, m, Ar). ¹³C NMR (75.4 MHz, CDCl₃): selected signals: 13.95 (C(O)OCH₂CH₃), 48.74 (CH), 49.04 (CH₂), 50.38 (CH₂), 51.48 (CH₂), 52.59 (CH₂), 52.95 (C(O)OCH₃), 53.62 (NCH₂CH), 53.62 (CH₂), 54.86 (CH₂), 54.96 (CH₂), 55.19 (CH₂), 55.37 (CH₂), 55.75 (CH₂), 56.18 (CH₂), 60.62 (CH₂), 60.94, 61.13, 61.21 (C(O)OCH₂), 127.83 (Ar), 128.12 (Ar), 128.41 (Ar), 131.53 (Ar), 131.84 (Ar), 132.62 (Ar), 167.79 (C(O), amide), 170.29 (2xC(O), ethyl ester), 170.52 (C(O), methyl ester), 170.91 (C(O), ethyl ester). HRMS (ESI): *m/z*: calcd for C₂₅H₃₉N₄O₇, [M+H]⁺, 507.2813, found: 507.2807.

Synthesis of 1-(4-Pyrenebutanamido)-carboxyethyl-4,7-bis-(ethoxycarbonylmethyl)-1,4,7-triaza cyclononane- tris-alkylated nonane 10: A solution of monoalkylated nonane **7** (0.69 g, 1.16 mmol) in trifluoroacetic acid in dichlorometane (60%, 25 mL) was stirred overnight at room temperature. The solvent was evaporated at reduced pressure. The residue was re-dissolved in dichlorometane and the solvent was evaporated. This procedure was repeated several times to give a light yellow thick oil. ¹H NMR spectroscopy (CDCl₃) revealed the disappearance of the signals assigned to the *Boc* group in precursor **7**. The oil (1.16 mmol, assuming quantitative deprotection) was dissolved in MeCN (30 mL), K₂CO₃ (1.6 g, 11.5 mmol) was added and the suspension was vigorously stirred at room temperature for 15 minutes. To this suspension was added ethyl bromoacetate (0.31 mL, 2.77 mmol). The suspension was vigorously stirred at room temperature overnight. The suspended solid was removed by filtration, the solvent was evaporated under reduce pressure and the residue was purified by flash chromatography (100% CH₂Cl₂ → CH₂Cl₂/EtOH (1:1)) to afford compound **10** (0.425 g, 55 %) as a white foam. ¹H NMR (300 MHz, CDCl₃): δ = 1.26 (m, 6 H, 2xC(O)OCH₂CH₃), 2.24 (m, 2 H, NHC(O)CH₂CH₂), 2.44 (m, 2 H, NHC(O)CH₂), 2.60-2.90 (m, 4 H, NCH₂C(O)), 2.50-3.40 (m, 16 H, N(CH₂)₂N, NCH₂C(O), NCH₂CH), 3.37 (m, 2 H, NHC(O)(CH₂)₂CH₂), 3.73 (s, 3 H, C(O)OMe), 3.92 (m, 4 H), 4.10 (m, 6 H, C(O)OCH₂), 4.81(d(br), 1 H, NCH₂CH), 7.80-8.40 (9 H, m, Ar). ¹³C NMR (75.4 MHz, CDCl₃): selected signals: 14.05 and 14.13 (C(O)OCH₂CH₃), 27.23 (NHC(O)CH₂CH₂), 32.67 (NHC(O)(CH₂)₂CH₂), 35.39 (NHC(O)CH₂), 43.50 (CH₂), 43.76 (CH₂), 43.98

(CH₂), 48.06 (CH₂), 51.22 (CH₂), 51.72(CH₂), 51.86 (C(O)OCH₃), 52.51 (CH), 52.60 (CH₂), 55.40 (CH₂), 55.64 (CH₂), 60.82, 60.98 (C(O)OCH₂), 123.63 (Ar), 124,62 (Ar), 124.75 (Ar), 124.85 (Ar), 125.76 (Ar), 126.51 (Ar), 127.18 (Ar), 127.41 (Ar), 127.46 (Ar), 128.67 (Ar), 129.72 (Ar), 130.87 (Ar), 131.32 (2xAr), 136.43 (C), 136.53 (Ar), 171.36 (C(O), ethyl ester), 171.39 (C(O), ethyl ester), 171.54 (C(O), methyl ester), 173.64 (C(O), amide).

Synthesis of fully deprotected ligands L₁, L₂ and L₃

Synthesis of aminocarboxyethyl-4,7-bis-(carboxymethyl)-1,4,7-triazacyclononane-fully deprotected NO₂A-N-(α -amino)propionic acid ligand (L₁): A solution of prochelator **8** (50 mg, 0.076 mmol) in a mixture hydrochloric acid 6M/ethanol (12 mL; 2/1 (v/v)) was stirred at room temperature for 2 hours. The solvent was evaporated under reduced pressure and the residue was re-dissolved in a mixture water/ethanol (10 mL; 1/1 (v/v)). The solution was adjusted to pH ~10 with Dowex-1X2100-OH⁻ resin (10 mL, wet resin) and the suspension was stirred for 1 hour at room temperature. The resin was transferred into a column, washed with water and further eluted with hydrochloric acid 0.1 M. The relevant fractions, identified by TLC (ethanol water 1/1, revelation with iodine vapor) were pooled together and evaporated at reduced pressure to afford ligand L₁ in the hydrochloride form as a off-white solid (25 mg, quantitative yield). ¹H NMR (300 MHz, D₂O): δ = 2.73-3.67 (m, 16 H, N(CH₂)₂N and NCH₂CO₂H), 3.06 (d, *J* = 3.9 Hz and x Hz, 1 H, ABX), 3.31 (dd, *J*= 12.3 and 3.9 Hz, 1 H, ABX), 5.01 (dd, *J*=10.5 and 3.9 Hz 1 H, ABX). ¹³C NMR (75.4 MHz, D₂O): 48.71 (CH₂), 49.04 (CH₂), 49.50 (CH₂), 50.93(CH₂), 51.68 (CH₂), 53.35 (CH), 57.31 (CH₂), 57.93 (CH₂), 58.46 (CH₂), 173.31 (CO₂H), 174.99 (CO₂H), 176.42 (CO₂H). HRMS (ESI) *m/z*: *calc*d for C₁₃H₂₅N₄O₆ [M+H]⁺: 333.1769, found: 333.1769.

Synthesis of benzamido-carboxyethyl-4,7-bis-(carboxymethyl)-1,4,7-triazacyclononane- fully deprotected NO₂A-N-(α -benzoylamido)propionic acid ligand (L₂): Prochelator (**9**) (323 mg, 0.89 mmol) was dissolved in a mixture ethanol/water (20 mL, 1/1 (v/v)). The solution was adjusted to pH ~10 by adding small portions of Dowex 1X2-100-OH⁻ resin. The suspension was stirred gently at room temperature for 2 hours. The wet resin was transferred into a chromatography column, washed with water (~50

mL) and eluted with hydrochloric acid 0.1 M. The relevant fractions, identified by TLC (ethanol water 1/1, revelation with iodine vapor) were pooled, concentrated at room temperature and further dried under vacuum to afford ligand **L**₂, in the hydrochloride form, as a light yellow solid (180 mg, 71 %). ¹H NMR (300 MHz, D₂O): δ= 2.9-3.6 (broad, overlapped signals with a integration corresponding to 14 H, N(CH₂)₂N and NCCH₂CH), 3.81 (broad, overlapped signals with a integration corresponding to 4 H, NCH₂CO₂H), 4.80 (m (broad), 1 H, CH), 7.53-7.88 (5 H, m, Ar). ¹³C NMR (75.4 MHz, D₂O): selected signals: 43.02 (CH₂), 48.11 (CH₂), 48.93 (CH₂), 49.03 (CH₂), 49.78 (CH₂), 51.39 (CH₂), 51.71 (CH), 51.91 (CH₂), 54.53 (CH₂), 56.08 (CH₂), 56.77 (CH₂), 127.46 (Ar), 129.04 (Ar), 132.60 (Ar), 133.32 (Ar), 170.20 (CO₂H), 177.17 (C(O), amide). HRMS (ESI): *m/z*: calcd for C₂₀H₂₉N₄O₇, [M+H]⁺, 437.2031, found: 437.2027.

Synthesis of 1-(4-Pyrenebutanamido)-carboxyethyl-4,7-bis-(carboxymethyl)-1,4,7-triazacyclononane- fully deprotected NO₂A-N-(α-pyrenebutanamido)propionic acid ligand (L₃): Prochelator (**10**) (0.360 g, 0.53 mmol) was dissolved in a mixture ethanol/water (1/1 v/v, 20 ml). The solution was adjusted to pH ~ 10 by adding small portions of Dowex 1X2-100-OH- resin. The suspension was kept under stirring at room temperature for 2 hours. The wet resin was transferred into a chromatography column, washed with water (~50 mL) and eluted with 0.1 M hydrochloric acid, followed by a mixture hydrochloric acid 0.2 M/ethanol (1/1 v/v). The relevant fractions, identified by TLC (ethanol/water, 1/1 v/v, revelation with iodine vapor and visualization under UV light λ₃₆₅ nm) were pooled, concentrated at room temperature and further dried under vacuum to afford deprotected chelator **L**₃ in the hydrochloride form, as a light yellow solid (0.149 g, 46 %). ¹H NMR (400 MHz, D₂O/CD₃OD): δ= 1.9-3.3 (broad, overlapped signals with a integration corresponding to 24 H, NHC(O)CH₂CH₂CH₂, NCH₂CO₂H, NCH₂CH and N(CH₂)₂N), 4.49 (m (br), 1 H, CH), 7.80-8.40 (9 H, m, Ar). ¹³C NMR (75.4 MHz, D₂O/CD₃OD): selected signals: 28.22 (NHC(O)CH₂CH₂), 33.25 ((NHC(O)(CH₂)₂CH₂), 36.23 ((NHC(O)CH₂), 48.92 (CH), 50.49 (CH₂), 54.95 (CH₂), 122.75 (Ar), 123.97 (Ar), 124.03 (CH-Ar), 124.58 (2x(CH-Ar)), 125.71 (CH-Ar), 126.19 (CH-Ar), 126.93 (C-Ar), 126.99 (CH-Ar), 127.28 (CH-Ar), 127.92 (CH-Ar), 129.24 (C-Ar), 130.20 (C-Ar), 130.70 (C-Ar), 135.44 (C-Ar), 171.98 (CO₂H), 172.19 (2xCO₂H), 175.41 (NHC(O)). HRMS (ESI): *m/z*: calcd for C₃₃H₃₈N₄NaO₇, [M+Na]⁺, 625.2638, found: 625.2621.

Preparation of Ga³⁺ chelates for ¹H and ⁷¹Ga NMR.

To an aqueous solution of ligand (pH = 3.0) was added dropwise an aqueous solution of the GaCl₃ in a 1:1 mole ratio. The pH was kept below 3.8 by the addition of aqueous NaOH. The solution was stirred at room temperature over night and the solvent was removed at reduced pressure. Solutions for NMR measurements (20 mM, D₂O) were obtained by dissolution of the solid complexes in D₂O (0.75 mL). ¹H and ⁷¹Ga NMR spectra of the complexes were obtained at 298 K on a Bruker Avance-3 400 Plus spectrometer, operating at 400.02 and 121.98 MHz, respectively. The proton NMR spectra of the complexes were assigned by 2D COSY and NOESY techniques using a Varian VNMRS 600 NMR spectrometer. The ¹H and ⁷¹Ga NMR pH study of the complexes was performed by adding small portions of NaOD or DCl to the complex solutions to obtain the desired pH.

Fluorescence Measurements

The absorption and the fluorescence emission spectra of the free ligand L₃ and the GaL₃ complex were recorded, respectively, with a Jasco V-630 UV-Vis spectrophotometer and a HORIBA JobinYvon Fluoromax-4 spectrofluorimeter, equipped with a monochromator in both excitation and emission and a temperature controlled cuvette holder. Fluorescence spectra were corrected for the instrumental response of the system. The fluorescence quantum yields (Φ_F) were determined using the standard method.^{52,53} Anthracene in ethanol ($\Phi_F = 0.27$)⁵⁴ was used as reference.

Radiochemistry

⁶⁷Ga³⁺ complexes for *in vivo* and *in vitro* experiments were prepared by adding 1 mCi of [⁶⁷Ga]citrate (produced at IBA Molecular, Louvain-la-Neuve) to a solution of 1 mg of the chelator in Hepes buffer (400 μ L, 0.4 M, pH 4) and heated at 80 °C for *ca* 1 hour. The radiochemical purity of the final products was determined by TLC. The percentage of bound metal was above 95% in all cases.

Calculation of log P

The lipophilicity of GaL₂ and GaL₃ complexes was assessed by computing their logP values using the **alops** software (free software available at <http://www.vclab.org/lab/alogsps>).⁵⁵

Stability in blood serum

For the blood serum stability studies, 5 µCi of a standard solution of [⁶⁷Ga]L₂ were added to 5 mL of fresh human serum, previously equilibrated in 5% CO₂ (95% air) environment at 37 °C. The mixture was kept in the same environment, and aliquots of 100 µL (in triplicate) were taken at appropriate periods of time (0 min, 30 min, and 1 hour). The aliquots were treated with 200 µL of ethanol, cooled (4 °C), and centrifuged during for 15 min at 4000 rpm, at 4 °C, in order to precipitate the serum proteins. A 100 µL aliquot of supernatant was collected for activity counting in a γ well-counter. The sediment was washed twice with 1 mL of EtOH and its activity was counted. The activity of the supernatant was compared to that of the sediment in order to determine the percentage of the chelate associated to the proteins. The activity of the supernatant at 1 hour was evaluated by TLC in order to check whether the chelate remained intact.

Biodistribution studies

All animal studies were performed by authorized researchers in strict adherence to the Portuguese law for animal protection.

Groups of four animals (Wistar male rats weighting *ca* 200 g) were anaesthetized with Ketamine (50.0 mg/mL)/chlorpromazine (2.5%) (10:3), injected in the tail vein with *ca* 100 µCi of [⁶⁷Ga]L₃ and sacrificed 1 and 24 hours later. The major organs were removed, weighted and counted in a γ well-counter. The biodistribution is stated as percentage of injected dose per gram of organ (%ID/g).

Acknowledgements

This work was financially supported by Fundação para a Ciência e Tecnologia, Portugal: PEst-C/UI0686/2013; FCOMP-01-0124-FEDER-037302; PTDC/UI/70063/2006; grant SFRH/BD/63994/2009 to Miguel Ferreira and sabbatical grant SFRH/BSAB/1328/2013 to J. A. Martins; Rede Nacional de RMN (REDE/1517/RMN/2005) for the acquisition of the Varian

VNMRS 600 NMR spectrometer at the University of Coimbra and the Bruker Avance-3 400 Plus at the University of Minho in Braga. We also acknowledge the COST Action TD1004 “Theragnostics Imaging and Therapy”.

Electronic Supplementary Information (ESI) available: 1D proton and 2D COSY NMR spectrum (600 MHz) of GaL₁ at pH 3.0 (Figure S1); 1D proton and 2D COSY NMR spectrum (600 MHz) of GaL₁ at pH 4.0 (Figure S2); UV-Vis spectra for the free ligand L₃ and the GaL₃ complex (1.0x10⁻⁵ M) (Figure S3); Fluorescence spectra for L₃ in non-deoxygenated water over the concentration range 1.0x10⁻⁷ and 5x10⁻³ mol.dm⁻³ (λ_{exc} = 345 nm) (Figure S4); Optimized structure of GaL₃ (Mopac PM6 COSMO water implicit solvent) (Figure S5). Computed logP for the GaL₂ and GaL₃ complexes after structure optimization with Mopac PM6 COSMO water implicit solvent (Table S1); Biodistribution, stated as percentage of injected dose per gram of organ (%ID/g), of ⁶⁷GaL₃ in Wistar rats at 1 and 24 hours after *i.v.* injection (Table S2).

References

- 1- Z. Li, P. S. Conti, *Adv. Drug Deliv. Rev.*, **2010**, *62*, 1031-51.
- 2- I. Kayani, A. M. Groves, *Clin. Med.*, **2006**, *6*, 240-244.
- 3- T. Ebenhan, M. Honer, S. M. Ametamey, P. A. Schubiger, M. Becquet, S. Ferretti, C. Cannet, M. Rausch, P. M. McSheehy, *Mol Imaging Biol.*, **2009**, *11*, 308-321.
- 4- F. Rösch, R. P. Baum, *Dalton Trans.*, **2011**, *40*, 6104-6111.
- 5- M. Fani, J. P. André, H. R. Mäcke, *Contrast Media Mol. Imaging*, **2008**, *3*, 53-63.
- 6- F. Rösch, P. J. Riss, *Curr. Top. Med. Chem.*, **2010**, *10*, 1633-1668.
- 7- M. I. M. Prata, *Curr. Radiopharmaceuticals*, **2012**, *5*, 142-149.
- 8- M. A. Green, M. J. Welsh, *Nucl. Med. Biol.*, **1989**, *16*, 435-448
- 9- S. Jurisson, D. Berning, W. Jia, D. Ma, *Chem. Rev.*, **1993**, *93*, 1137-1156.
- 10- T. J. Wadas, E. H. Wong, G. R. Weisman, C. J. Anderson, *Chem. Rev.*, **2010**, *110*, 2858-2902.
- 11- W. R. Harris, V. L. Pecoraro, *Biochemistry*, **1983**, *22*, 292-299.
- 12- V. Kubicek, J. Havlicková, J. Kotek, G. Tircsó, P. Hermann, É. Tóth, I. Lukes, *Inorg. Chem.*, **2010**, *49*, 10960-10969.
- 13- A. F. Martins, M. I. M. Prata, S. P. J. Rodrigues, C. F. G. C. Geraldés, P. J. Riss, A. Amor-Coarasa, C. Burchardt, C. Kroll, F. Rösch, *Contrast Media Mol. Imaging*, **2013**, *8*, 265-273.
- 14- M. Bauwens, R. Chekol, H. Vanbilloen, G. Bormans, A. Verbruggen, *Nucl. Med. Comm.*, **2010**, *31*, 753-758.
- 15- D. A. Moore, P. E. Fanwick, M. J. Welch, *Inorg. Chem.*, **1990**, *29*, 672-676
- 16- E. T. Clarke, A. E. Martell, *Inorg. Chim. Acta*, **1991**, *181*, 273-280.
- 17- C. J. Broan, J. P. L. Cox, A. S. Craig, R. Katakya, D. Parker, A. Harrison, A. M. Randall, G. Ferguson, *J. Chem. Soc. -Perkin Trans. 2*, **1991**, 87-99.
- 18- J. -F. Morfin, É. Tóth, *Inorg. Chem.*, **2011**, *50*, 10371-10378.
- 19- D. J. Hnatowich, P. Schiegel, *J. Nucl. Med.*, **1981**, *22*, 623-626.
- 20- J. Schuhmacher, R. Matys, H. Hauser, W. Maierborst, S. Matzku, *Eur. J. Nucl. Med.*, **1986**, *12*, 397-404.
- 21- R. Delgado, F. M. de Carmo, S. Quintino, *Talanta*, **1997**, *45*, 451-462
- 22- R. M. Smith, A. E. Martell, *Critical Stability Constants*, Plenum Press, New York, 1989.
- 23- A. Heppeler, S. Froidevaux, H. R. Mäcke, E. Jermann, M. Béhé, P. Powell, M. Hennig, *Chem. Eur. J.*, **1999**, *5*, 1974-1981.

- 24- A. Heppeler, J. P. André, I. Buschmann, X. Wang, J.-C. Reubi, M. Hennig, T. A. Kaden, H. R. Mäcke, *Chem. Eur. J.*, **2008**, *14*, 3026-3034.
- 25- I. Velikyan, H. Mäcke, B. Langstrom, *Bioconjugate Chem.*, **2008**, *19*, 569-573.
- 26- A. de Sá, A. A. Matias, M. I. M. Prata, C. F. G. C. Geraldes, P. M. T. Ferreira, J. P. André, *Biorg. & Med. Chem. Let.*, **2010**, *20*, 7345-7348.
- 27- J. P. André, H. R. Mäcke, M. Zehnder, L. Macko, K. G. Akyel, *Chem. Commun.*, **1998**, 1301-1302.
- 28- K. P. Eisenwiener, M. I. M. Prata, I. Buschmann, H. W. Zhang, A. C. Santos, S. Wenger, J. C. Reubi, H. R. Mäcke, *Bioconjugate Chem.*, **2002**, *13*, 530-541.
- 29- J. Notni, P. Hermann, J. Havlíčková, J. Kotek, V. Kubiček, J. Plutnar, N. Loktionova, P. J. Riss, F. Rösch, I. Lukes, *Chem. Eur. J.*, **2010**, *16*, 7174-7185.
- 30- J. Šimeček, M. Schulz, J. Notni, J. Plutnar, V. Kubiček, J. Havlíčková and P. Hermann, *Inorg. Chem.*, **2012**, *51*, 577-590.
- 31- J. Šimeček, J. Notni, V. Kubiček and P. Hermann, *Nucl. Med. Biol.*, **2010**, *37*, 679.
- 32- A. N. Singh, W. Liu, G. Hao, A. Kumar, A.O. Z O. K.Gupta, J.- T. Hsieh, X. Sun, *Bioconjugate Chem.*, **2011**, *22*, 1650-1662.
- 33- M. Studer, C. F. Meares, *Bioconjugate Chem.*, **1992**, *3*, 337-341.
- 34- M. F. Ferreira, A. F. Martins, J. A. Martins, P. M. Ferreira, É. Tóth, C. F. G. C. Geraldes, *Chem. Commun.*, **2009**, 6475-6477.
- 35- M. F. Ferreira, B. Mousavi, P. M. Ferreira, C. I. O. Martins, L. Helm, J. A. Martins, C. F. G. C. Geraldes, *Dalton Trans.*, **2012**, *41*, 5472-5475.
- 36- M.F. Ferreira, A.F. Martins, C.I.O Martins, P.M. Ferreira, É Tóth, T.B. Rodrigues, D. Calle, S. Cerdan, P. Lopez-Larrubia, J.A. Martins, C.F.G.C. Geraldes, *Contrast Media Mol. Imaging*, **2013**, *8*, 40-49.
- 37- M. F. Ferreira, G. Pereira, A. F. Martins, C. I. O. Martins, M. I. M. Prata, S. Petoud, E. Toth, P. M. T. Ferreira, J. A. Martins, C. F. G. C. Geraldes, *Dalton Trans.*, **2014**, *43*, 3162-3173.
- 38- J. W. Akitt, in *Multinuclear NMR*, Ed. J. Mason, Plenum press, New York, Chapter 9, pp. 259-288.
- 39- L. Ronconi, P. J. Sadler, *Coord. Chem. Rev.*, **2008**, *252*, 2239-2277.
- 40- a) J. P. André, H. R. Mäcke, *J. Inorg. Biochem.*, **2003**, *97*, 315-323; b) J. P. André, NMR Spectroscopy of Gallium in Biology, in "Encyclopedia of Metalloproteins", R. H. Kretsinger, V. N. Uversky, E. A. Permyakov (Eds.), Springer, 2013

- 41- A. S. Craig, D. Parker, H. Adams, N. A. Bailey, *J. Chem. Soc., Chem. Comm.*, **1989**, 1793-1794.
- 42- D. Shetty, S. Y. Choi, J. M. Jeong, L. Hoigebazar, Y.-S. Lee, D. S. Lee, J.-K. Chung, M. C. Lee, Y. K. Chung, *Eur. J. Inorg. Chem.*, **2010**, 5432-5438.
- 43- M. I. M. Prata, A. C. Santos, C. F. G. C. Geraldés, J. J. P. de Lima, *J. Inorg. Biochem.*, **2000**, 79, 359-363.
- 44- C. J. Broan, K. J. Jankowski, R. Kataký, D. Parker, *J. Chem. Soc. Chem. Comm.*, **1990**, 1738-1739.
- 45- A. de Sá, M. I. M. Prata, C. F. G. C. Geraldés, J. P. André, *J. Inorg. Biochem.*, **2010**, **104**, 1051-1062.
- 46- F. M. Winnik, *Chem. Rev.* **1993**, 93, 587-614.
- 47- S. J. A. Pope, *Polyhedron*, **2007**, 26, 4818-4824.
- 48- J. P. Holland, V. Fisher, J. A. Hickin, J. M. Peach, *Eur. J. Inorg. Chem.*, **2010**, 48-58.
- 49- C. Wang, S. D. Wettig, M. Foldvari, R. E. Verrall, *Langmuir*, **2007**, 23, 8995-9001.
- 50- C. Keyes-Baig, J. Duhamel, S. Wettig, *Langmuir*, **2011**, 27, 3361-3371.
- 51- P. K. Glasoe, F. A. Long, *J. Phys. Chem.*, **1960**, 64, 188-189.
- 52- J. N. Demas, G. A. Crosby, *J. Phys. Chem.*, **1971**, 75, 991-1024.
- 53- S. Fery-Forgues, D. Lavabre, *J. Chem. Educ.*, **1999**, 76, 1260-1264.
- 54- J. V. Morris, M. A. Mahaney, J. R. Huber, *J. Phys. Chem.*, **1976**, 80, 969-974.
- 55- I. V. Tetko, J. Gasteiger, R. Todeschini, A. Mauri, D. Livingstone, P. Ertl, V. A. Palyulin, E. V. Radchenko, N. S. Zefirov, A. S. Makarenko, V. Y. Tanchuk, V. V. Prokopenko, *J. Comput. Aid. Mol. Des.*, **2005**, 19, 453-463.